

ON THE USE OF EDDY RESOLVING TECHNIQUES TO SIMULATE RIVER TRANSPORT PROCESSES AND FLOW AROUND HYDRAULIC STRUCTURES

George Constantinescu¹

ABSTRACT

This paper describes recent efforts under way at the IIHR-Hydroscience and Engineering related to the use of eddy resolving and advanced near-wall modeling techniques to simulate flow around hydraulic structures and associated pollutant / sediment transport phenomena. Sample results obtained using a Large Eddy Simulation (LES) fully three-dimensional (3D) non-hydrostatic non-dissipative massively parallel solver that can use hybrid unstructured grids are reported for three cases: 1) flow in a channel with a circular bridge pier; 2) flow and mass exchange processes around two spur dikes containing an embayment; 3) flow inside a pump intake of realistic geometry. Additionally, results obtained using a recently developed Detached Eddy Simulation (DES)/RANS fully three-dimensional non-hydrostatic model to solve for the flow, free surface deformation, bed / suspended load sediment transport and bed morphology changes in open channel flows and river reaches that can account for roughness effects and does not use wall functions are presented. In these preliminary RANS simulations the equilibrium scour configuration and associated sediment transport are predicted for the flow in a curved open channel with loose bed. The overall goal of the present research effort is to use eddy resolving techniques (e.g., LES, DES) as a predictive tool that can be employed in the design, optimization and control process of the flow past hydraulic structures and to predict the transport processes within open channels and river reaches.

1. INTRODUCTION

The presence of massive separation and the associated vortex shedding, as well as unsteady intermittent meandering vortices is a common feature of many river engineering applications including flow around hydraulic structures and flow in river reaches of complex geometry in which the flow is highly 3D. Even sophisticated RANS models are known to fail in these flows. Accurate simulations of these flows require the use of modeling approaches like LES that can resolve at least the energetically most important eddies in the flow and model only the remaining ones. In turn, controlling the amount of numerical dissipation present in these codes is essential to obtain accurate results. The purpose of these studies is not only to predict the statistics of these flows more accurately than the classical approaches using RANS models, but also to use the information from

¹ Assistant Professor, Civil & Environmental Engineering, IIHR-Hydroscience and Engineering, The University of Iowa, Stanley Hydraulics Laboratory, Iowa City, IA 52242--1527, USA. Phone: 1-319-384-0630 Fax: 1-319-335-5238 Email: sconstan@engineering.uiowa.edu

the 3D instantaneous flow fields to understand the fundamental physics of these flows, in particular the role played by the main coherent structures. The other common feature of the studies discussed

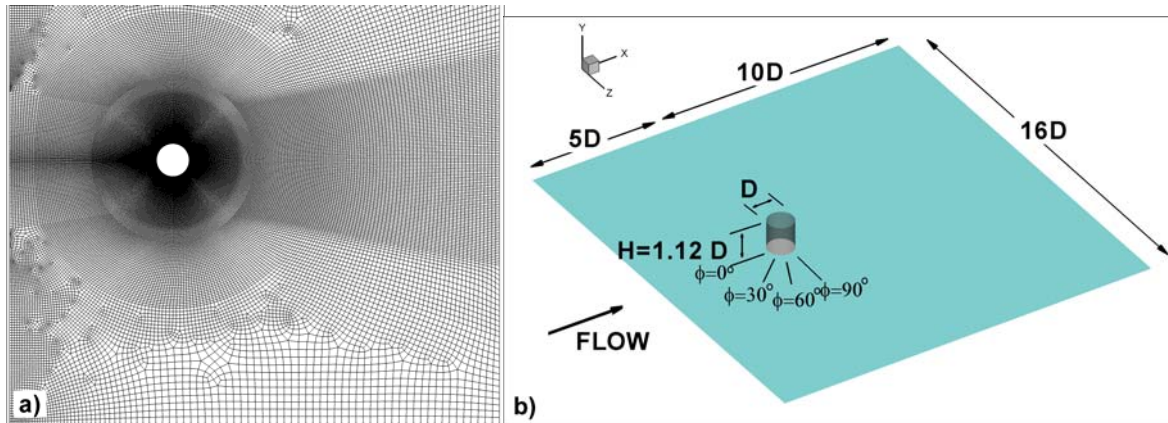


Figure 1 Unstructured mesh and computational domain for bridge pier mounted on a flat bed.

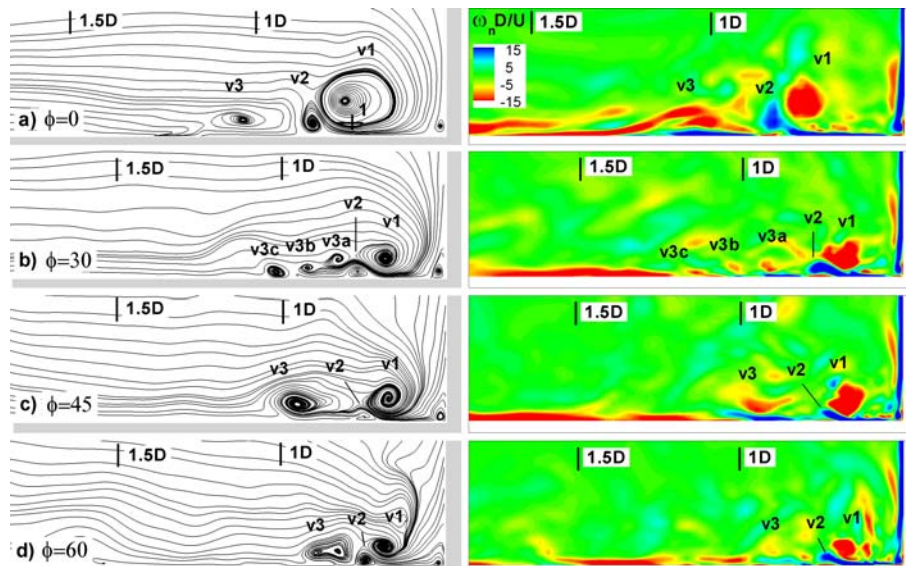


Figure 2 Instantaneous streamlines and out-of-plane vorticity contours showing instantaneous horseshoe vortex system. a) $\phi=0^\circ$; b) $\phi=30^\circ$; c) $\phi=45^\circ$; d) $\phi=60^\circ$; e) $\phi=90^\circ$ plane.

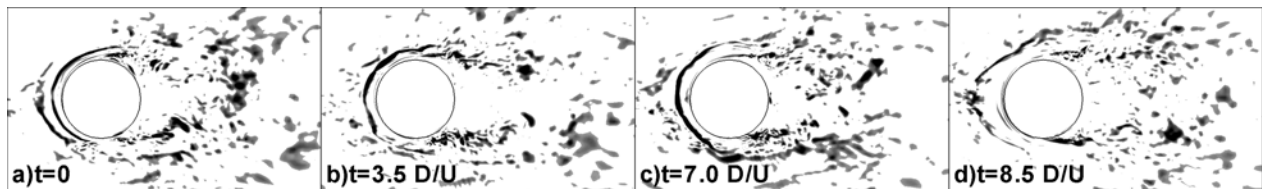


Figure 3 Time evolution of in-plane instantaneous vorticity contours in $y/D=0.04$ plane.

in this paper is the use of near wall models which do not assume the validity of the law of the wall near solid surfaces, as is the case with the widely used wall function models. At the same time these models can account for roughness effects. These two aspects are essential in improving the predictive capabilities of the CFD models used for river applications.

2. LES SIMULATIONS OF FLOW AROUND HYDRAULIC STRUCTURES

The numerical solver utilized in the present examples of flow around complex hydraulic structures is a massively parallel LES code (Mahesh, Constantinescu and Moin, 2004) that allows simulating flow in complex geometries using unstructured hybrid meshes. A collocated, finite volume scheme is used to solve the filtered Navier-Stokes equations with a dynamic Smagorinsky model. An advantage of the dynamic Smagorinsky model is that it does not require any special treatment (e.g.,

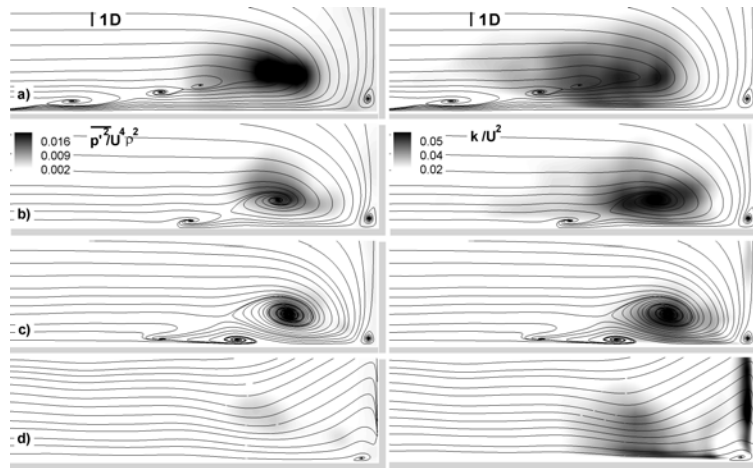


Figure 4 R.m.s. of pressure fluctuations and resolved t.k.e. a) $\phi=0$; b) $\phi=30$; c) $\phi=60$; d) $\phi=90$ plane.

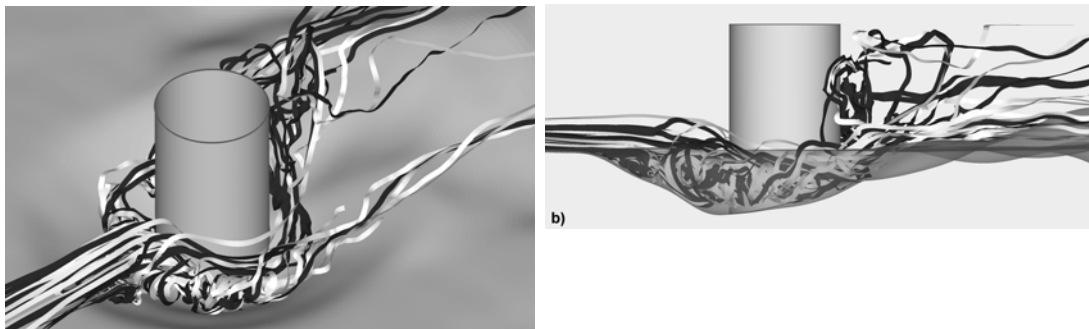


Figure 5 Three dimensional streamtraces inside the scour hole. a) perspective view; b) side view.

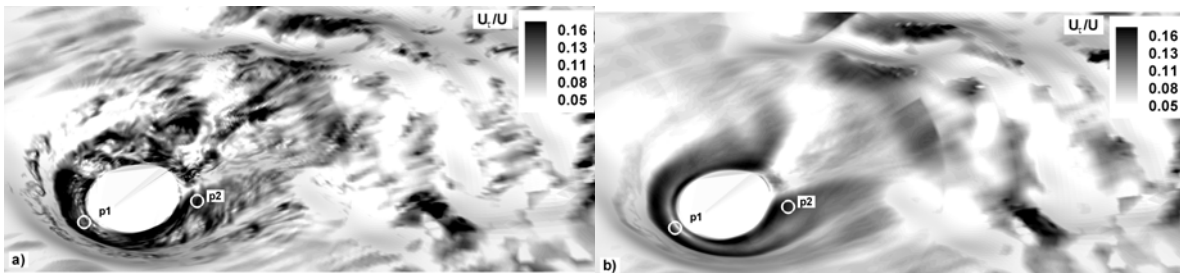


Figure 6. Bed friction velocity contours for equilibrium scour case. a) instantaneous; b) mean.

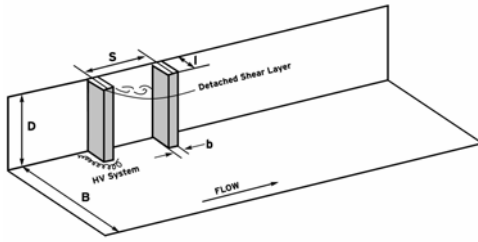


Figure 7 General sketch of flow in a channel with two lateral obstructions.

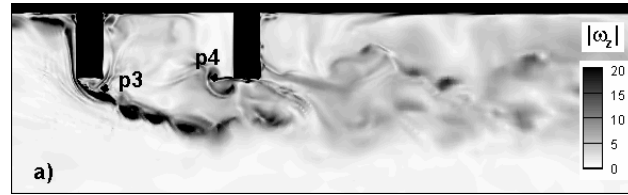


Figure 8 Instantaneous contours of out-of-plane vorticity magnitude in the free surface plane

damping functions) in the near wall region and has no adjustable constants. The algorithm is non-dissipative yet robust at high Reynolds numbers on highly skewed meshes. Discrete energy conservation was found essential to ensure this behavior. Central schemes are used to discretize the operators, including the convective terms and no filtering of the resolved velocity field is used.

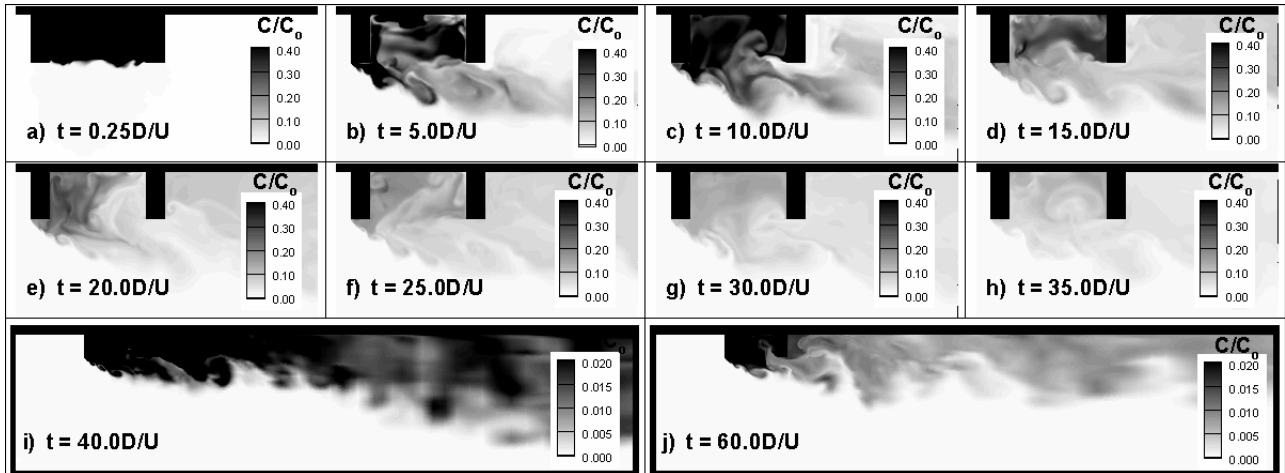


Figure 9 Time evolution of passive scalar concentration in embayment and channel. Mixing starts at $t=0D/U$ when the concentration in the embayment is set to $C/C_0=1.0$.

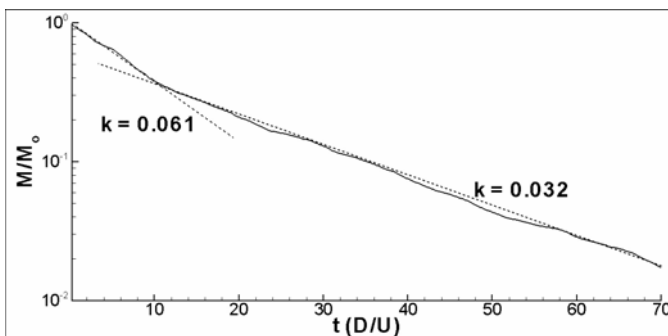


Figure 10 Scalar mass decay within embayment.

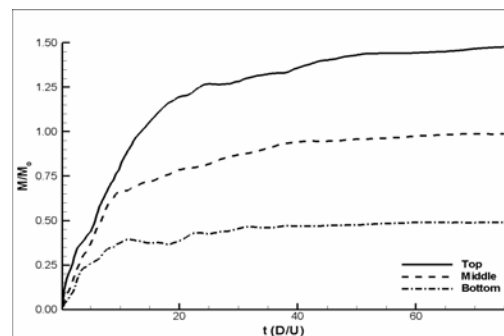


Figure 11 Mass transport into main channel corresponding to the top, middle and bottom third sections of embayment-channel interface

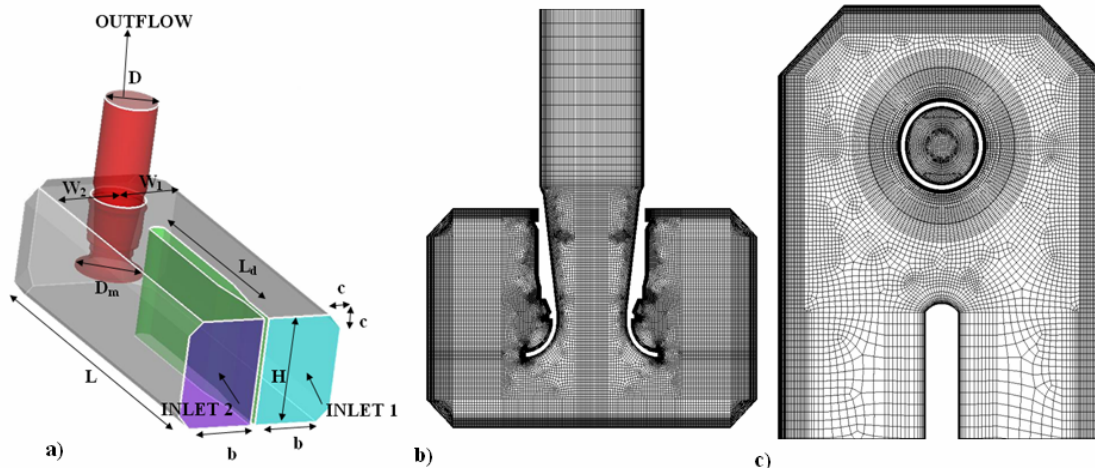


Figure 12 Pump-intake geometry. a) General sketch of the pump-sump; b) Mesh in a section parallel to the back wall; c) Mesh in a section close to the pump bell level.

As a first example results from the simulation of the flow around a circular bridge pier ($Re_D=18,000$) with fully developed incoming turbulent flow and flat bed corresponding to initiation of the scouring process are presented. More details can be found in Kirkil et al. (2005a). Figure 1 shows a section through the unstructured mesh containing over 4 million cells along with a sketch of computational domain. The focus of the study was to investigate the mechanism responsible for the scour initiation and the spatio-temporal structure of the horseshoe vortex (HV) system at the base of the cylinder. As observed in Figures 2 and 3, the HV system is not formed of structures that wrap more or less uniformly around the cylinder as is the case when the HV system is laminar. Rather the main eddies that are part of the HV system extend over very variable distances in the polar direction around the upstream part of the pier and are continuously and randomly created and destroyed. All this creates very large variations in the structure, position, size and overall intensity of the turbulent HV system in the case of a flat bed when the HV system is not stabilized by the presence of the scour hole. As expected, the regions characterized by large values of the bed shear stress are situated beneath the eddies associated with the HV system and the detached shear layers where very energetic vortex tubes are shed at a high frequency. The largest values are recorded for polar angles larger than 30° very close to the junction which explain why the scour is initiated on the sides of the cylinder in the case of a loose flat bed. As also observed in experimental investigations, our simulation confirms that the HV region is characterized by large velocity and pressure fluctuations (see Figure 4). Same flow, but at the end of the scouring process, was studied by Kirkil et al. (2005b). The deformed bed bathymetry was obtained from experiments. An overall view of the HV region inside the scour hole is shown in Figure 5. It is found that the bed shear stress fluctuations around the local mean values can be very high, especially in the scour and near wake regions (Figure 6). The mean flow fields show that for the given conditions, the mean HV system contains one primary eddy close to the cylinder. Inside this eddy the pressure fluctuations and resolved t.k.e. levels are very high. The largest mean bed shear stress levels (Figure 6b) are observed beneath this eddy as well as close to the small corner vortex at the base of the cylinder.

A second example is the simulation of flow and contaminant removal from the embayment area (Figure 7) between two vertical groynes in a channel (McCoy et al., 2005a, 2005b). The upstream flow is fully turbulent. The mass transfer is simulated using a passive (conserved) scalar transport equation. The vortical structures that populate the detached shear layer (Figure 8) and their interaction with the recirculation eddies inside the embayment area and with eddies originating at the tip of the downstream obstruction that entrain fluid from the region downstream of the second

groyne inside the embayment are shown to play an important role in the pollutant entrainment from the groyne area into the main channel. The evolution of the concentration field in time shown in Figure 9 describes the dispersion process of the pollutant cloud as it is convected downstream of the groyne area. The decay of pollutant within the embayment was quantified enabling calculation of a global 1D exchange coefficient, k , based on dead-zone theory. It was found that the exchange process is not characterized by a unique value of k . Rather, as shown in Figure 10, two distinct phases of the decay process were identified. In the initial phase of decay over which about 68% of the total mass of pollutant leaves the embayment, the exchange coefficient was found to be about twice the value recorded for the final phase. LES also allowed a detailed quantification of the non-uniformity of the exchange process over the depth of the embayment. It was found that in the later stages of the mixing part of the pollutant entrained outside the embayment through the middle / top layers does not originate in these layers but rather is convected from the bottom region (Figure 11). The process is highly 3D and the bottom of the embayment acts toward delaying the mass exchange.

A third example is the simulation of the flow in a pressurized pump intake of complex geometry (Tokuy and Constantinescu, 2005a, 2005b). The presence of unsteady intermittent meandering wall attached and free-surface vortices is a common feature of pump intake flows. These vortices are known to induce high levels of unsteady swirl inside the pump column and negatively affect the performance of the pumps. The model is validated using the PIV data collected on a scaled model by Yulin et al. (2000). The grid contained close to 5 million cells (Figure 12). To better put in perspective the predictive performances of LES, results from simulations employing the SST RANS model are also included. Overall, LES statistics showed better agreement with experimental data than RANS. If the velocity fields and mean streamlines patterns were captured

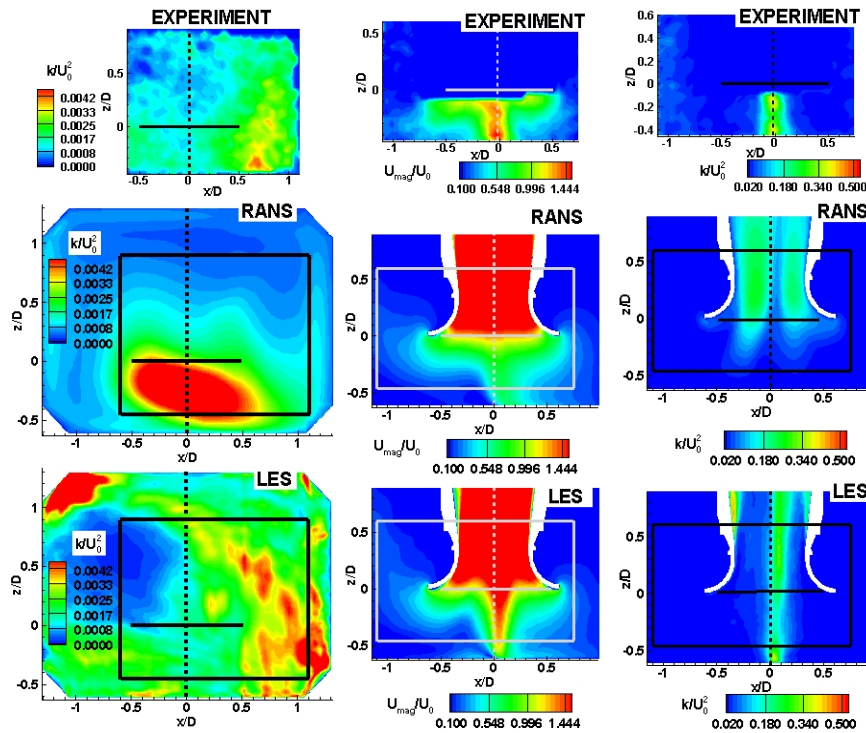


Figure 13 Contours of velocity magnitude and turbulent kinetic energy (t.k.e.) at different sections.

- a) T.k.e. - $y1$ plane situated at $0.4D$ from backwall; b) Velocity magnitude - $y3$ plane cutting through center of pump column; c) T.k.e. - $y3$ plane.

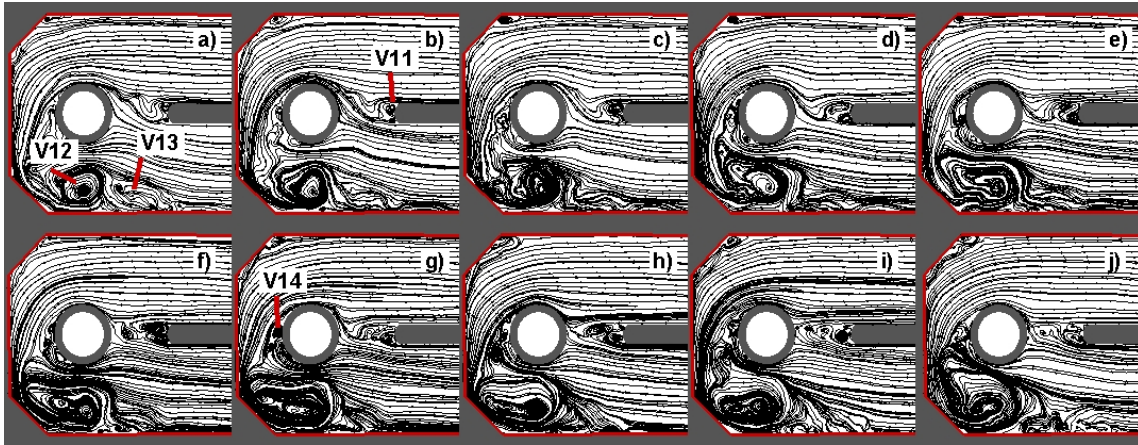


Figure 14 Instantaneous streamlines in a plane parallel to the channel floor situated at $1.13D$ from floor a) $t = 0$; b) $t = 15D/U$; c) $t = 30D/U$ d) $t = 45D/U$; e) $t = 60D/U$; f) $t = 75D/U$; g) $t = 90D/U$; h) $t = 105D/U$; i) $t = 120D/U$; j) $t = 140D/U$.

rather satisfactory by the RANS simulation, RANS failed quite dramatically in predicting the turbulent kinetic energy (t.k.e.) distribution throughout the flow (Figure 13), in particular in the region where the floor attached vortex, which was the strongest coherent structure in the flow, was present. It is also found that some of the vortical structures are meandering or are intermittent. For instance, Figure 14 visualizes the temporal variation in the structure of a vertical vortex (V12) parallel to the pump column as well as the unsteady shedding taking place behind the cylinder and downstream the tip of the dividing wall between the two approach channels. The meandering of the floor attached vortex along with its variations in strength and mean diameter are quantified in Figure 15. This study shows that LES can be used to obtain detailed information on the evolution and interactions among the main vortices that is very hard to obtain from scaled model studies. Maybe

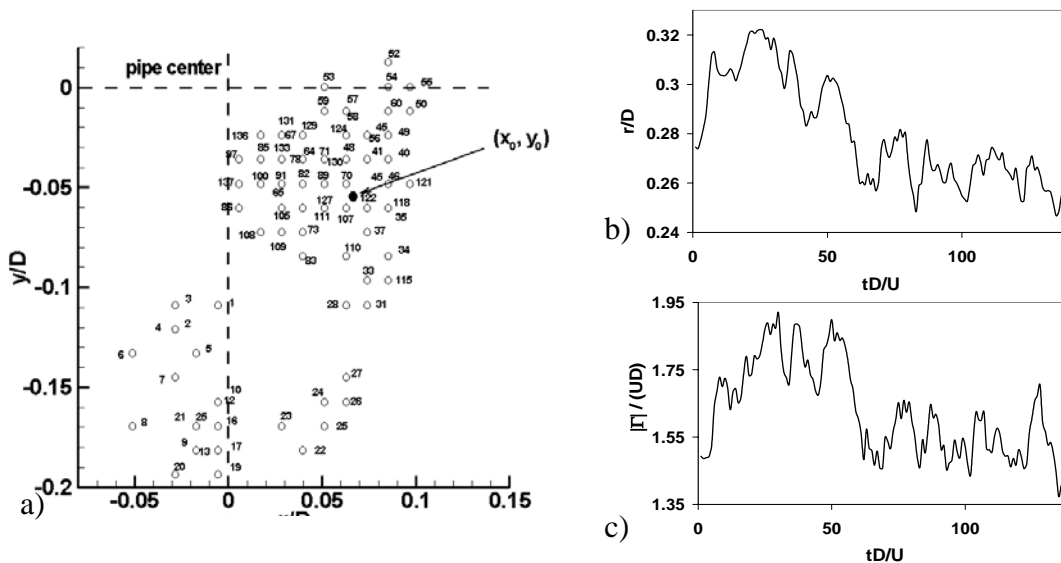


Figure 15 Evolution of floor attached vortex in a section situated at $0.2D$ from the floor. a) Position of core center; b) Mean core radius; c) Absolute circulation.

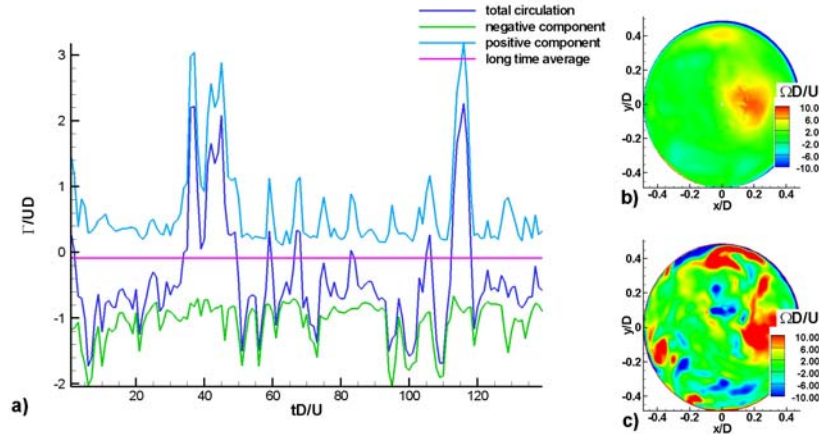


Figure 16 Circulation inside the pump column in a plane 2.0D from pump bell level; a) Evolution of circulation in time; b) Mean out-of-plane vorticity; c) Instantaneous out-of-plane vorticity.

the most important quantity is the value of swirl present in the pump column close to the pump levels. A major advantage of LES over RANS is that it provides continuous swirl (circulation) data at any level inside the pump column which can be used to study the time evolution of the swirl. In many cases the performance of the pumps is adversely affected not only by the mean value of the swirl (circulation) which can also be obtained from RANS (though the accuracy of the prediction will be most probably lower) but also by its level of unsteadiness which is not available from a steady RANS simulation. Figure 16 shows the time variation of the total circulation inside the pump column in a section situated at 2.0D from the pump bell level, along with the positive and negative components of the total swirl. The horizontal line corresponds to the long time average. What is interesting to remark is not only the fact that the total circulation displays large variations around the mean values but also that it changes sign pretty regularly. We intend to use this CFD model as a tool to test new design ideas or to optimize the shape of various vortex suppressing devices.

3. SIMULATION OF FLOW IN CURVED OPEN CHANNELS WITH MOVABLE BEDS

A newly developed (Zeng et al., 2005a, 2005b, Constantinescu and Squires, 2004) non-hydrostatic fully 3D model that solves the incompressible, RANS equations in generalized curvilinear coordinates is used to predict flow through straight and meandering open channels, including sediment transport. The model integrates the equations up to the wall such that the use of wall-functions is avoided. The model can use the Spalart-Allmaras (SA) and $k-\omega$ models in near-wall versions that can account for bed roughness effects. The choice of the turbulence models is partly motivated by the fact that in the next phase of the study DES will be used. DES is a hybrid method in which the base RANS model is modified in the regions away from the solid boundaries such that it acts as a LES model allowing the eddy viscosity to scale with the square of the local grid spacing as in classical LES. The solver uses movable grids in the vertical direction to account for changes in the free surface elevation where the proper kinematic and dynamic conditions are imposed and in the bathymetry due to erosion / deposition at the bed as the code converges toward equilibrium scour configuration. A non-equilibrium bed load sediment transport model similar to the one used by Wu et al. (2000) is used with the additional introduction of down-slope gravitational force effects. The suspended sediment is modeled using an advection diffusion equation with a settling velocity term. To our knowledge this is the first time the coupling between the suspended load and

the bed load layers is done in the context of using near-wall models in a fully 3D code, in which the first point off the wall is situated well within the thickness of the bed load layer. Validation of the deformable free surface and suspended sediment modules is accomplished through simulation of test cases in straight channels (Zeng et al., 2005a, 2005b). The model is then used to predict the suspended and bed loads as well as the equilibrium bed bathymetry through an 180° open channel bend (Figure 17) for which detailed experimental data are available. The simulations started with a flat sand bed. Two simulations using SA model were performed on a grid with 360,000 mesh points. In the first one only the bed load transport was considered, as this component was observed to be the main mode of sediment transport in the experiment, while in the second one both the bed

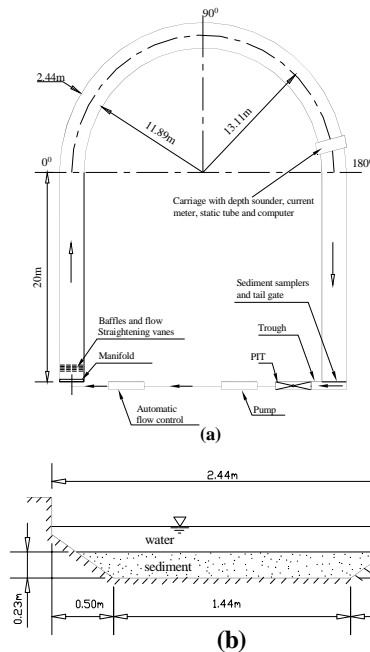


Figure 17. Sketch of Odgaard & Bergs experiment. (a) experiment layout; (b) cross-section of the flume.

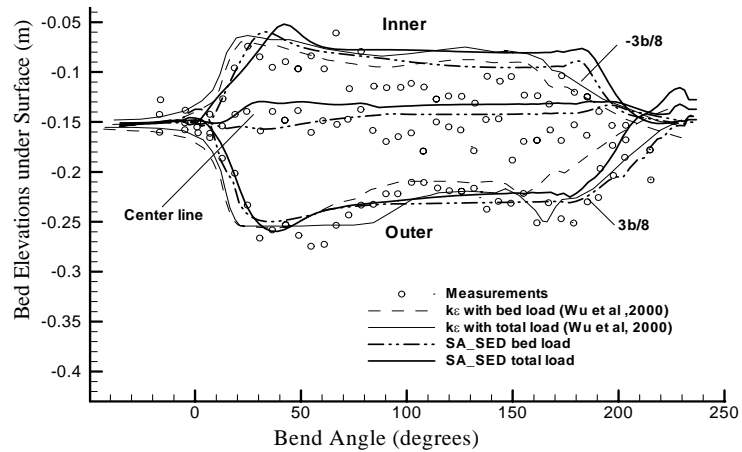


Figure 18. Comparison of longitudinal water depth at three positions in the channel bend.

load and the suspended load transport were considered. To better assess the performance of the model, results obtained using the $k-\epsilon$ model with wall functions by Wu et al. (2000) are also included. Figure 18 shows the variation of the water depth along the streamwise direction (θ) at three positions situated at $3b/8$ (near outer bank), 0 and $-3b/8$ (near inner bank) from the centerline for the simulations and experiment. In Figure 19 the simulated equilibrium channel cross sections at five representative locations ($0^\circ < \theta < 180^\circ$) are compared with the measurements and the $k-\epsilon$ simulation. The water level is situated at the zero mark in all cross sections. As expected, the largest depths are observed near the outer bend. Near the inner bank deposition takes place and a short sand bar is present. Both SA_SED and $k-\epsilon$ simulations appear to satisfactorily capture the variations of the water depth and bed elevation inside the bend. However, some differences can be observed. With the exception of the fact that the SA_SED simulation that accounts for the suspended sediment predicts very accurately the maximum depth and its position in the $\theta=45^\circ$ section, the SA_SED simulation that takes into consideration only the bed load appears to produce slightly better agreement with the measurements in the sections represented in Figure 20. The largest error present in the $k-\epsilon$ simulation results are observed near the inner bank in the $\theta=0^\circ$ section where the model predicts the formation of a sandbar way too early compared to the experiments and to the SA_SED simulations. Overall, the performance of the newly developed model in predicting

this complex test case was quite satisfactory, with both SA_SED simulations predicting relatively close results. Results obtained using $k-\omega$ model showed similar level of agreement.

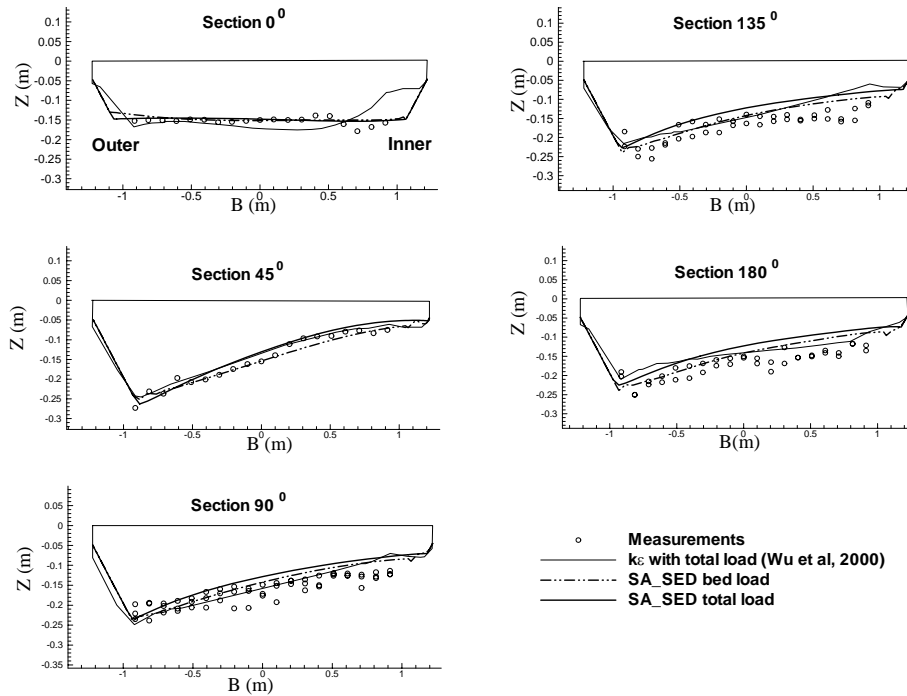


Figure 19 Comparison of bed levels between simulations and measurement results.

4. CONCLUSIONS

The present simulations demonstrate that a non-dissipative LES model using fine enough meshes can effectively complement the information obtained from experimental studies toward understanding the complex flow and mixing phenomena present in flows around hydraulic structures. Moreover, the statistics calculated from LES appear to be closer to the experimental data compared to results using RANS simulations conducted on very fine meshes and without using wall functions. A parallel effort that tries to develop a DES solver to predict movable bed flows is under way. Versions of the SA and $k-\omega$ models without wall functions that can account for roughness effects were implemented into a URANS/DES solver. Though for meandering open channels in which massive separation was not present, the RANS simulations using the newly proposed model showed only a slight improvement over simulations using 3D RANS models with wall functions, it is expected that when applied to flows characterized by massive separation (e.g., scour around hydraulic structures like bridge piers / abutments or spur dikes) the use of near wall RANS and especially DES models will give more accurate hydrodynamics predictions and, ultimately, sediment predictions compared to RANS models that use wall functions. This is because the underlying assumptions associated with the wall function approach are not satisfied in these flows. Similar LES / DES modeling efforts are under way to study gravity driven flows and mass exchange processes involving dense miscible contaminants for various river engineering applications.

REFERENCES

Constantinescu, S.G. and Squires, K.D. (2004). "Numerical investigation of the flow over a sphere in the subcritical and supercritical regimes," *Physics of Fluids*, Vol. 16, pp. 1449-1467.

- Kirkil, G., Constantinescu, S.G. and Ettema, R. (2005a), "The horseshoe vortex system around a circular bridge pier on a flat bed," XXXIst International Association Hydraulic Research Congress, Seoul, Korea, September 2005.
- Kirkil, G., Constantinescu, S.G., and Ettema, R. (2005b), "The horseshoe vortex system around a circular bridge pier on equilibrium scoured bed," World Water and Environmental Resources Congress, Alaska, May 2005.
- Mahesh, K., Constantinescu, S.G. and Moin, P. (2004). "A numerical method for large eddy simulation in complex geometries," J. Computational Physics, Vol. 197, No. 1, pp. 215-240.
- McCoy, A., Constantinescu, S.G. and Weber, L. (2005a), "LES simulation of contaminant removal from the embayment area between two vertical groynes in a channel," XXXIst International Association Hydraulic Research Congress, Seoul, Korea, September 2005.
- McCoy, A., Constantinescu, S.G. and Weber, L. (2005b), "Coherent structures and mass exchange processes in channel flow with spanwise obstructions," ERCOFTAC International Symposium on Engineering Turbulence Modeling and Measurements, Sardinia, Italy, May 2005.
- Tokyay, T. and Constantinescu, S.G. (2005a), "Large Eddy Simulation and Reynolds Averaged Navier Stokes Simulations of flow in a realistic pump intake: A validation study," World Water and Environmental Resources Congress, Alaska, May 2005.
- Tokyay, T. and Constantinescu, S.G. (2005b), "Coherent structures in pump intake flows: A Large Eddy Simulation study," XXXIst International Association Hydraulic Research Congress, Seoul, Korea, September 2005.
- Yulin, W., Yong, L. and Xiaoming L., (2000), "PIV Experiments on flow in a model pump suction sump." Research Report, Tsinghua University, China.
- Wu, W., Rodi, W. and Wenka, T. (2000), "3D numerical modeling of flow and sediment transport in open channels," J. Hydraulic Engineering, ASCE, 126, pp. 4-15.
- Zeng, J., Constantinescu, S.G. and Weber, L. (2005a), "A fully 3D non-hydrostatic models for prediction of flow, sediment transport and bed morphology in open channels," XXXIst International Association Hydraulic Research Congress, Seoul, Korea, September 2005.
- Zeng, J., Constantinescu, S.G. and Weber, L. (2005b), "Validation of a computational model to predict suspended and bed load sediment transport and equilibrium bed morphology in open channels," River and Coastal Estuarine Morphology Conference, University of Illinois, 2005.